The Journal of Experimental Biology 204, 3507–3522 (2001)
Printed in Great Britain © The Company of Biologists Limited 2001
JEB3534

The effects of speed on the *in vivo* activity and length of a limb muscle during the locomotion of the iguanian lizard *Dipsosaurus dorsalis*

Frank E. Nelson* and Bruce C. Jayne

Department of Biological Sciences, PO Box 210006, University of Cincinnati, Cincinnati, OH 45221-0006, USA

*Present address: Oregon State University, Zoology Department, 3029 Cordley Hall, Corvallis, OR 97331-2914, USA (e-mail: nelsonfr@ava.bcc.orst.edu)

Accepted 18 July 2001

Summary

The caudofemoralis muscle is the largest muscle that inserts onto the hindlimb of most ectothermic tetrapods, and previous studies hypothesize that it causes several movements that characterize the locomotion of vertebrates with a sprawling limb posture. Predicting caudofemoralis function is complicated because the muscle spans multiple joints with movements that vary with speed. Furthermore, depending on when any muscle is active relative to its change in length, its function can change from actively generating mechanical work to absorbing externally applied forces. We used synchronized electromyography, sonomicrometry and three-dimensional kinematics to determine *in vivo* caudofemoralis function in the desert iguana *Dipsosaurus dorsalis* for a wide range of speeds of locomotion from a walk to nearly maximal sprinting (50–350 cm s^{-1}). Strain of the caudofemoralis increased with increasing tail elevation and long-axis rotation and protraction of the femur. However, knee extension only increased caudofemoralis strain when the femur was protracted. The maximum and minimum length of the caudofemoralis muscle and its average shortening velocity increased from the slowest speed up to the walk–run transition, but changed little with further increases in speed. The times of muscle shortening and lengthening were often not equal at higher locomotor speeds. Some (20–25 ms) activity occurred during lengthening of the caudofemoralis muscle before footfall. However, most caudofemoralis activity was consistent with performing positive mechanical work to flex the knee shortly after foot contact and to retract and rotate the femur throughout the propulsive phase.

Key words: terrestrial, locomotion, muscle, electromyography, sonomicrometry, physiology, kinematics, lizard, *Dipsosaurus dorsalis.*

Introduction

During steady locomotion when muscles are loaded cyclically, differences in the timing of muscle activity and the length of the contractile tissue allow muscle and tendon together to function in three ways: to generate positive work, to generate negative work or to act as a spring (Biewener, 1990). For example, the anterior myomeric musculature of fish is electrically active mainly when the muscle shortens and flexes the fish towards the side of muscle activity that generates positive work (for a review, see Rome, 1994). In contrast, the posterior myomeric musculature of fishes often has substantial electrical activity during lengthening and, hence, may perform negative work that stiffens the body to retard bending movements away from the side of muscle activity (Altringham et al., 1993). Similarly, negative work performed by limb muscles can prevent a limb joint from collapsing (Abraham and Loeb, 1985) or decelerate an oscillating appendage (Full et al., 1998). If the contractile tissue of muscle generates sufficient force to become stiffer than the tendon, then the tendon can act like a spring by lengthening and shortening *via* elastic recoil, as in the gastrocnemius muscle of running turkeys (Roberts et al., 1997) and hopping wallabies (Biewener et al., 1998b).

In addition to these differences in muscle function, in many species of animal, limb function during locomotion may also be affected by differences in posture. Compared with birds and mammals, lizards and salamanders have a more sprawling limb (Ashley-Ross, 1994a; Ashley-Ross, 1994b; Edwards, 1977; Hildebrand, 1985; Rewcastle, 1981; Sukhanov, 1974). In contrast to most endothermic vertebrates, the movements of sprawling vertebrate limbs involve substantial long-axis rotation of the femur and femur retraction in a horizontal plane (Brinkman, 1981; Jayne and Irschick, 1999; Rewcastle, 1981). However, the posture and movements of the hindlimb in some ectothermic vertebrates change as the limb becomes increasingly erect with increasing speed (Jayne and Irschick, 1999).

Many of the hindlimb movements that characterize vertebrates with sprawling limbs are probably caused by the caudofemoralis muscle (CF). The CF is the single largest hindlimb muscle in many species of ectothermic tetrapod, and

such a large size implies an important locomotor function. For example, in generalized species of iguanian lizard, the CF often makes up more than 20 % of the entire mass of the hindlimb musculature and is 2–4 times more massive than the next largest hindlimb muscle (Snyder, 1954). In salamanders (Ashley-Ross, 1995; Peters and Goslow, 1983), lizards (Reilly, 1995) and crocodilians (Gatesy, 1990; Gatesy, 1997), the electrical activity of the CF is correlated with retraction of the femur while the foot contacts the ground (stance). Snyder's (Snyder, 1962) stimulation of the isolated CF in both lizards and alligators caused femur retraction, and the extent of femur rotation and knee flexion depended on the angle of femur retraction. Available data for lizards (Brinkman, 1981; Irschick and Jayne, 1999a; Jayne and Irschick, 1999) indicate that femur retraction and rotation occur nearly simultaneously during stance, and these kinematic variables together with knee flexion change significantly with increasing locomotor speed (Jayne and Irschick, 1999). However, no previous study of CF function in ectothermic tetrapods has quantified either femur rotation or any effects of locomotor speed.

Understanding the function of the CF is complicated because the muscle spans more than one joint. The CF of all ectothermic tetrapods originates from several caudal vertebrae and inserts *via* a short stout tendon on the ventral and proximal portion of the femur. A unique feature of saurian reptiles (lizards and crocodilians) is a long, thin auxiliary tendon that runs parallel to the femur and attaches to the joint capsule of the knee (Fig. 1). Consequently, the auxiliary tendon could stretch when the muscle is active. Furthermore, three-dimensional methods are required to measure both femur rotation and knee flexion for a sprawling limb. For steady terrestrial locomotion of tetrapods, simultaneous measurements of *in vivo* muscle activity and length are only available for a few endothermic species (Abraham and Loeb, 1985; Biewener et al., 1998b; Carrier et al., 1998; Roberts et al., 1997). Such data are lacking for the CF and all other locomotor muscles of ectothermic tetrapods.

In this study, we determined the three-dimensional hindlimb movements and *in vivo* activity and length changes of the CF in *Dipsosaurus dorsalis* during steady terrestrial locomotion over a wide range of speeds from a walk to a nearly maximal sprint (50–350 cm s^{-1}). Besides gaining general insights into how the limb muscles function during the terrestrial locomotion of animals, we were interested in testing the following specific hypotheses. We hypothesized that the maximum length of the caudofemoralis in *D. dorsalis* would increase with increasing speed because the overall amounts of femur protraction, femur rotation and knee extension increase with increasing speed (from 50 to 250 cm s^{-1}) (Jayne and Irschick, 1999). The duration of the stance phase of *D. dorsalis* decreases significantly with increased speed (Fieler and Jayne, 1998; Jayne and Irschick, 1999). Consequently, we hypothesized that the shortening velocity of the CF would increase with increasing speed. We also wanted to compare our *in vivo* values of muscle shortening velocity with those that may maximize power on the basis of Hill's (Hill, 1938) ratio of shortening to maximal velocity for isotonic tetanic contractions and values determined for cyclical loading using work loops (Askew and Marsh, 1998; Johnson et al., 1993; Swoap et al., 1993).

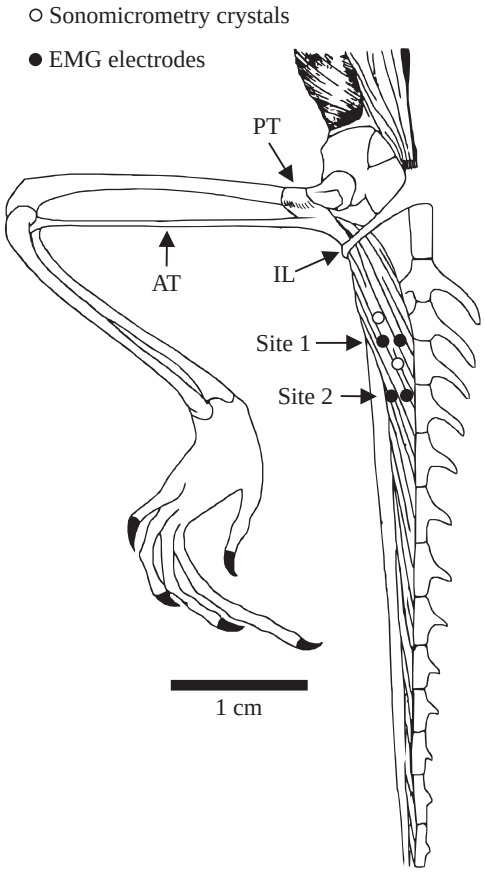

Fig. 1. Ventral view of the caudofemoralis muscle of the right hindlimb of *Dipsosaurus dorsalis* with the illiocaudalis and ishiocaudalis removed. The symbols indicate the approximate longitudinal and lateral locations of electromyographic (EMG) electrodes and sonomicrometry crystals. Electrodes were implanted at two sites. AT and PT indicate the auxiliary and primary tendons of the caudofemoralis muscle, respectively, and IL is the illioischiadic ligament.

Materials and methods

Experimental subjects

The desert iguana *Dipsosaurus dorsalis* is useful for studying hindlimb function because it moves over a large range of locomotor speeds and has a generalized hindlimb morphology relative to some other terrestrial species of lizard (Fieler and Jayne, 1998). Furthermore, extensive background data exist for *D. dorsalis* for both the limb movements (Irschick and Jayne, 1999b; Jayne and Ellis, 1998) and the *in vitro* physiology of different muscle fiber types (Gleeson, 1983; Gleeson and Dalessio, 1990; Gleeson et al., 1993; Gleeson and Johnston, 1987; Gleeson et al., 1980; Marsh and Bennett, 1985; Marsh and Bennett, 1986). The caudofemoralis

(CF) muscle of adult *D. dorsalis* is sufficiently large to accommodate several electromyographic (EMG) electrodes and sonomicrometry crystals. Thus, this system is well-suited for a study of *in vivo* function. All of the five individuals that we used for statistical analyses were adults with mean (± S.E.M.) values of snout–vent length and mass of 12.1±0.3 cm (range 11.3–12.4 cm) and 45±4 g (range 34–55 g), respectively.

Experimental protocol

We used Halothane to anesthetize all animals before implanting sonomicrometry crystals and electromyographic (EMG) electrodes. Animals were allowed to recover from anesthesia for 2–4 h before being placed on a variable-speed motorized treadmill. *Dipsosaurus dorsalis* were run for 30–60 s on the treadmill after their body temperature had reached 37–40 °C, which is similar to the average field active body temperatures (40 °C) of this species (Johnston and Gleeson, 1984). Rest periods between trials varied from 15 to 60 min. We attempted to obtain data for seven standardized steady speeds ranging from 50 to 350 cm s^{-1} in 50 cm s^{-1} increments. We defined steady-speed locomotion as that for which the change in average forward velocity of successive strides varied by less than 10 %. The order in which lizards were run at different speeds was randomized to minimize any confounding effects of time on the effects of speed. After each experiment, the lizard was killed, and radiographs and dissection were used to determine the position of sonomicrometry crystals and EMG electrodes.

We obtained simultaneous dorsal and lateral views of the lizards using a two-camera NAC HSV-500 high-speed video system operating at 250 images s^{-1}. Video recordings were synchronized with EMG and sonomicrometry recordings using a 100 Hz square-wave generator that provided output to both the video system and EMG and sonomicrometry tape recordings. Paint marks on the pelvis, on the hindlimb and at intervals of 2–3 vertebrae along the mid-dorsal line of the tail facilitated digitization of the video images. The most proximal paint mark on the tail had approximately the same longitudinal position as the sonomicrometry crystals.

For three lizards, we also tested the effects of isolated movements and combinations of movements on the length of the caudofemoralis *in vivo*. Immediately after implantation, we placed the deeply anesthetized lizard on an apparatus to manipulate the hindlimb. We retracted, rotated and depressed the femur, as well as flexed and extended the knee, independently and in various combinations, to determine the effects on muscle length.

Electromyography and sonomicrometry

We used fine-wire bipolar electrodes to record the *in vivo* activity of the muscle, and the general methods of constructing bipolar EMG electrodes followed those of Jayne (Jayne, 1988). We used 0.051 mm diameter polycoated stainless-steel wire (California Fine Wire Co., USA) with approximately 0.7 mm of insulation removed from the recording end. A ground wire was also implanted in the epaxial musculature of the tail. After implantation, we used cyanoacrylate glue to attach electrode wires to the skin of the lizard's tail and plastic model cement to glue together the two wires of each electrode and all electrodes together into a single cable. The lengths of wire from the animals to the probes of the recorder was approximately 2 m, which was long enough to allow the lizard to move freely. We implanted a total of four EMG electrodes into the longus head of the right CF (Fig. 1).

To measure *in vivo* muscle length, we implanted two 0.7 mm diameter piezoelectric crystals (Sonometrics Corp.). After cutting through the skin of the anesthetized lizard, the fascia between the illiocaudalis and the ischiocaudalis muscles was separated to expose the CF. The sonomicrometry crystals were then placed in separate small incisions (1 or 2 mm deep) in the CF parallel to the orientation of the muscle fibers approximately 6 mm apart and between the second and fourth caudal vertebrae (Fig. 1). We used cyanoacrylate glue to secure the sonomicrometry crystals within the muscle. One EMG electrode was placed in the muscle between the two crystals while the incision was open (site 1). We used 4-0 silk suture to close the incision and hold the wire leads of the sonomicrometry crystals in place. We then percutaneously implanted three additional EMG electrodes. One electrode was placed 1–2 vertebrae caudal to the first electrode (site 2). The remaining two electrodes were implanted at the same longitudinal positions as sites 1 and 2 but lateral to the previously implanted electrodes (Fig. 1).

Electromyograms (EMGs) were amplified 5000× using Grass P511k series amplifiers with high- and low-bandpass filters of 100 Hz and 10 kHz, respectively, and a 60 notch filter. The analog EMG and sonomicrometry signals were recorded at 9.5 cm s^{-1} using a Teac XR-7000 FM data recorder. We converted the analog signals to digital data using a Keithley 500A analog-to-digital converter with an effective sampling rate of 8 kHz (Jayne et al., 1990b). Digital EMGs were filtered using a high-pass finite-impulse response filter to reduce the amplitude of the signal below 100 Hz to less than 10 % of the original amplitude.

We used a customized computer program (written by Garr Updegraff, San Clemente, CA, USA; garru@uci.edu, garru@fea.net) to measure onset and offset times (± 1 ms) and the rectified integrated area (area) for each burst of muscle activity. The following EMG variables were calculated for all CF sites: EMG duration (emgdur=offset minus onset), EMG intensity (intensity=area/emgdur) and EMG duty factor (emgdur cycle/duration). To facilitate the pooling of data from different individuals, we divided each value of intensity per burst by the maximal value of intensity observed within each individual over the entire range of speeds (50–350 cm s^{-1}), and the resulting values of relative intensity were expressed as percentages.

Eleven variables described the magnitude and timing of changes in length of the muscle. For each locomotor cycle, we determined the maximum (L_{max}) and minimum (L_{min}) length of contractile tissue between the sonomicrometry crystals and the times at which these lengths occurred (TL_{max} and TL_{min}).

We used the average of L_{max} and L_{min} at the slowest speed (50 cm s^{-1}) to estimate resting length (L_0). To facilitate the pooling of muscle length data among individuals (with minor differences in initial crystal position), we converted L_{max} and L_{min} to relative changes in length (ΔL_{max} and ΔL_{min}) by subtracting L_0 and expressing the result as a percentage of L_0. Net percentage strain per cycle (ΔL_{net}) equaled $\Delta L_{max}-\Delta L_{min}$. Average shortening velocity (V) was $\Delta L_{net}/(TL_{max}-TL_{min})$. The percentage of each cycle spent lengthening ($\%T_{lengthen}$) was calculated as ($TL_{min}-TL_{max}$)/(cycle duration), where cycle duration was the time between successive beginnings of swing phase (foot above the tread surface). At slow speeds, once L_{min} had been attained, the length often remained at L_{min} for a substantial period; therefore, the percentage of the cycle spent shortening ($\%T_{shorten}$) was calculated using the difference between TL_{max} and the subsequent earliest time of L_{min} (TL_{min}). Consequently, the sums of $\%T_{lengthen}$ and $\%T_{shorten}$ were frequently less than 100 %.

Nine variables related the timing of changes in muscle length to muscle activity and kinematics. We calculated the lag times between the times of maximum and minimum muscle length relative to the beginning ($Lag_{Lmax-on}=TL_{max}-$onset) and end ($Lag_{Lmin-off}=TL_{min}-$offset) of the electrical activity of the muscle, respectively. The lag times between TL_{max} and the times of footfall ($Lag_{Lmax-down}$), maximum femur protraction ($Lag_{Lmax-fempro}$), maximum anterior femur rotation ($Lag_{Lmax-antrot}$) and maximum knee extension near footfall ($Lag_{Lmax-kext}$) were calculated as TL_{max} minus kinematic timing variable. Similarly, the lag times between L_{min} and the times of foot-up ($Lag_{Lmin-up}$), maximum femur retraction ($Lag_{Lmin-femret}$) and maximum posterior rotation ($Lag_{Lmin-pstrot}$) were calculated as TL_{min} minus kinematic timing variable. For all these lag times, positive values indicate that the first event indicated in the subscript occurred after the second event listed in the subscript.

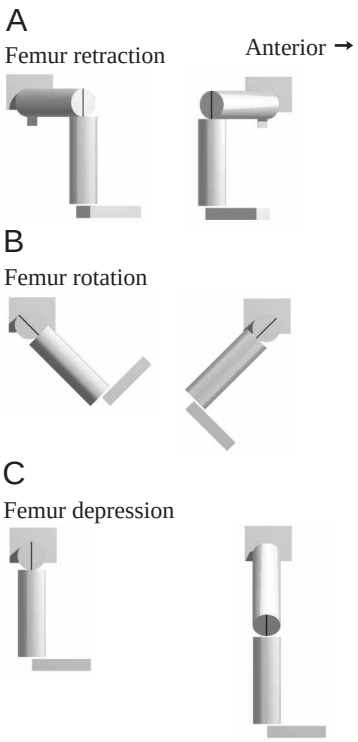

Fig. 2. A schematic right lateral view of major movements of the right femur. The most dorsal rectangular box represents the pelvis. The long cylinder attached to the pelvis is the femur. The small rectangle on the femur represents the greater trochanter, which is parallel to the black reference line on the distal end of the femur. The more distal cylinder represents the lower leg, and the most ventral rectangle represents the tarsals and metatarsals. For each pair of figures in a row, the figure on the right illustrates the movement relative to the initial position shown on the left. For the sake of simplicity, rotation of the pelvis in the horizontal plane is not shown, but this movement occurs in most lizards and salamanders.

Kinematics

The duration of the stance and swing phases (stancedur, swingdur) were the time elapsed within each stride when the right hind foot touched or was above the tread surface, respectively, and the sum of these two quantities was the cycle (stride) duration (stridedur). Cycle frequency equaled 1/stridedur. The kinematic duty factor (stancedur/stridedur) was expressed as a percentage of the cycle duration.

We used customized video-analysis software (Stereo Measurement TV, written by Garr Updegraff, San Clemente, CA, USA; garru@uci.edu, garru@fea.net) to digitize all the two- and three-dimensional coordinates. Depending on the stride duration, images were digitized at either 4 or 8 ms intervals, resulting in 20–40 images for each stride. For the three-dimensional coordinate system, the x-axis was horizontal and parallel to the overall direction of travel and the motion of the tread surface, the y-axis was perpendicular to the tread, and the z-axis was perpendicular to the x,y plane. We digitized the three-dimensional coordinates of the following landmarks painted on the animal: the right pelvic landmark, knee and ankle and two points on the mid-dorsal line of the proximal tail. We also digitized the two-dimensional coordinates of the left pelvic landmark (x,z) and a point on the mid-dorsal line of the neck (x,y). Several other variables, including two- and three-dimensional angles, were calculated from coordinates using macros for Microsoft Excel version 7.0 (written by G. Updegraff and B. C. Jayne).

Before calculating the kinematic quantities, we transformed the coordinates of the pelvic landmarks to approximate the coordinates of the hip (as in Jayne and Irschick, 1999) by correcting for the vertical and horizontal distance from the pelvic landmarks to the hip joint on the basis of measurements from preserved specimens. We could not reliably measure the amount of pelvic roll about the longitudinal axis of the lizard because the right hip generally obscured the view of the left hip, which was needed to determine its y-coordinate (Jayne and Irschick, 1999). Consequently, we determined certain movements of the femur relative to fixed planes of reference. The angle of femur retraction (Fig. 2A) was a two-dimensional angle determined from a dorsal view of the femur and the line

connecting the left and right hips, so a value of 0° indicated when the femur was perpendicular to the longitudinal axis of the pelvis, and greater magnitudes of positive and negative values indicated greater amounts of retraction and protraction, respectively. The angle of femur rotation about its long axis (Fig. 2B) was a three-dimensional angle between the plane containing the femur and the tibia and a vertical reference plane passing through the femur, so larger positive values indicated greater clockwise (posterior) rotation of the right femur in a right lateral view. The angle of femur depression (Fig. 2C) was a three-dimensional angle between the femur and a horizontal plane passing through the right hip, so positive and negative values indicated that the femur was below or above the horizontal reference plane through the hip, respectively. The angle between the femur and the tibia, the knee angle, was calculated such that smaller values between 0 and 180° indicate greater flexion of the joint.

The tail dorsal angle was a two-dimensional (*x*,*y*) angle determined from the line segments connecting the third caudal vertebra (proximal tail paintmark) to the pelvic landmark and from the pelvic landmark to a point on the mid-dorsal line of the neck. Greater magnitudes of positive and negative values indicated more elevated and depressed tail positions, respectively. We used the dorsal view to determine the two-dimensional (*x*,*z*) tail lateral angle as the angle between the line segments representing the most proximal segment of the tail (from the most proximal tail paintmark to a point midway between the left and right pelvic landmarks) and the longitudinal axis of the pelvis (through the pelvic midpoint). Positive and negative values of tail lateral angle indicated that the base of the tail pointed to the right and left, respectively. We estimated tail lateral flexion in the region of the sonomicrometry crystals by determining the two-dimensional (*x*,*z*) angle between the most anterior tail segment (from the pelvic midpoints to the first paintmark) and the second most anterior tail segment (from the first to the second paint mark). Positive and negative values of tail lateral flexion indicated the tail was concave to the right and left, respectively.

Statistical analyses

Although EMG electrodes and sonomicrometry crystals were implanted in 11 lizards, we were only able to obtain balanced data sets suitable for analysis of variance (ANOVA) for a subset of these individuals. Qualitatively, the data from all individuals appeared grossly similar. Some descriptive statistics are provided for trials at a speed of 350 cm s^{-1}; however, all ANOVAs were restricted to six speeds ranging from 0 to 300 cm s^{-1}. The measurements used in all ANOVAs were from 2–4 strides per individual per speed.

One individual used for ANOVAs of EMG data lacked muscle-length data, and two individuals used for ANOVAs of muscle-length data lacked accompanying EMG data. Two additional individuals were used for ANOVAs of all types of data. Consequently, ANOVAs were performed on three groups of variables for which the number of individuals (N_i) was as follows: (i) EMGs only (N_i=3), (ii) lag times between EMGs and length change (N_i=2) and (iii) length changes and their timing relative to kinematics (N_i=4). We used SYSTAT version 5.0 (Wilkinson, 1992) to perform a two-way mixed-model ANOVA for which speed was a fixed factor (N=6) and individual was a random factor. Consequently, the F-ratio for the main effect of speed was the mean square for speed divided by the mean square for the speed × individual interaction term (Zar, 1999). The criterion for statistical significance was $P \leqslant 0.05$.

Unless stated otherwise, the mean values for each speed presented in the text and graphics for descriptive purposes are given ± S.E.M. and were calculated on the basis of the number of strides (N_s) pooled across all individuals at a particular speed. Depending on the particular variable, mean values were from a different numbers of individuals (N_i). As emphasized above, one should rely on the ANOVA results for the tests of statistical significance since only these methods properly account for the repeated-measures experimental design.

To clarify whether the effects of speed on EMG and muscle-length variables were similar among different individuals, we calculated least-squares regressions with both linear and quadratic polynomials of speed including data from 350 cm s^{-1} when they were available. To clarify how kinematics were related to muscle length, we also calculated multiple regressions using kinematic data (pooled from all individuals) as the independent variables and muscle-length variables as the dependent variables.

Results

Morphology

The caudofemoralis longis muscle of *Dipsosaurus dorsalis* originates from the third to thirteenth caudal vertebrae and inserts *via* a thick tendon near the greater trochanter of the femur, and an auxiliary tendon extends to the distal part of the knee joint capsule that attaches to the proximal portion of the crus (Fig. 1). The proximal portions of both tendons of the caudofemoralis pass through the illioischiadic ligament, which forms a loop on the pelvis (Fig. 1).

Electromyography and sonomicrometry

The locomotor speeds for which EMGs were detectable for different electrodes implanted in a single caudofemoralis muscle varied considerably (Fig. 3), and this implied substantial spatial heterogeneity in the distribution of the different fiber types. For example, only one of the three electrodes for which data are shown in Fig. 3 (1M) had substantial activity over the entire range of speeds from 50 to 350 cm s^{-1}. Other electrodes detected little substantial activity until locomotor speeds exceeded 150 cm s^{-1} (Fig. 3, 2M) or 250 cm s^{-1} (Fig. 3, 1L). For two electrodes at the same longitudinal position (site 1) and for all speeds of the same individual shown in Fig. 3 (1M, 1L), the EMG onset from the electrode that detected activity only at the faster locomotor speeds lagged significantly behind that from the electrode that detected activity at slower locomotor speeds (mean paired

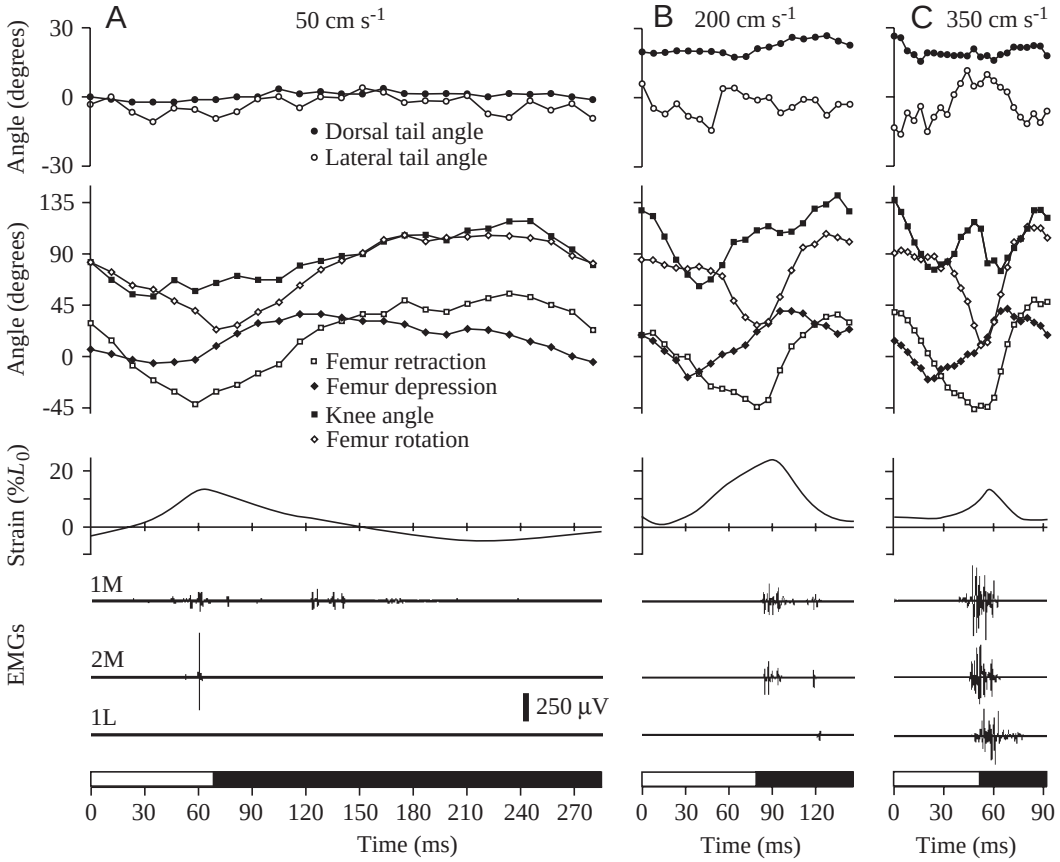

Fig. 3. Angles of the tail and hindlimb, and strain and electromyograms from the caudofemoralis muscle, for one stride cycle for one individual of *Dipsosaurus dorsalis* at each of three speeds 50 cm s^{-1} (A), 200 cm s^{-1} (B) and 350 cm s^{-1} (C). The muscle strain is expressed as a percentage change from resting length (L_0). The elapsed time within each stride shown at the bottom of each panel starts and ends at the beginning (foot-up) of the swing phase (white bar), and the black bar indicates the duration of the stance phase after footfall. The numerals to the left of each electromyogram indicate the longitudinal positions of three different electromyograms electrodes within a single muscle (see Fig. 1), and M and L indicate the medial and lateral locations within a longitudinal position, respectively.

difference ± 95 % CL=20±11 ms, where CL is confidence limit, N_s=13, N_i=1). Furthermore, the magnitude of the lag time between onsets of these regions with different threshold locomotor speeds for recruitment decreased significantly with increasing speed (r=–0.69, P=0.009, N_s=13, N_i=1). In contrast to the variable onset times from different regions of the muscle, the lag time between EMG offsets was neither significantly different from zero nor significantly correlated with speed. The relationships between the timing of EMG activity from regions with different threshold locomotor speeds for recruitment were statistically similar for a second individual. Additional results only use data from the region of the muscle within each individual that had the lowest threshold locomotor speed for recruitment, and these regions were defined operationally as the slower fiber type on the basis of differences in EMGs stated above. Thus, we chose electromyographic data to pool across individuals that would minimize the effects of different fiber types and for which data would be available for the slowest standardized speeds.

As locomotor speed decreased from 300 to 50 cm s^{-1}, the values of both EMG duration and cycle duration showed an approximately threefold increase (Table 1) that was highly significant (Table 2). Because of the nearly proportional decreases in EMG duration and cycle duration with increasing speed, EMG duty factor did not change significantly with speed (Table 2; Fig. 4A), and the grand mean for data pooled across all individuals and speeds was 34 %. As shown in Fig. 3, the amplitudes of EMGs generally increased with increasing locomotor speed, and the ANOVA of relative intensity confirmed that this trend was significant (Table 2). The increases in relative intensity were most conspicuous and consistent as speed increased from 50 to 200 cm s^{-1} (Table 1). Although the relative intensity of some individuals increased over the entire range of increased locomotor speed, other individuals showed little apparent change in relative intensity from 200 to 350 cm s^{-1}.

Both maximum (ΔL_{max}) and minimum (ΔL_{min}) muscle strain changed significantly with locomotor speed (Table 3) such that values increased regularly with increasing speed up to a value between 150 and 200 cm s^{-1}, whereupon little change was apparent for further increases in speed (Fig. 4B). The significant speed by individual interaction terms for ΔL_{max} and ΔL_{min} (Table 3) partly reflect that the muscle strains of one individual increased linearly with increasing speed, whereas

Table 1. *Descriptive statistics of electromyographic and length variables*

Variable	N_i	Speed (cm s^{-1}) 50	100	150	200	250	300	350
Cycle duration (ms)	3	253±14	177±11	152±5	134±5	114±6	103±6	96±4
Kinematic duty factor (%)	3	68±2	60±2	53±1	49±2	46±2	45±3	40±3
EMG duration (ms)	3	106±10	61±6	47±5	36±4	39±3	29±3	33±4
Relative intensity (% of maximum)	3	17±1	32±5	37±7	62±10	49±10	61±10	70±6
$Lag_{Lmax–on}$ (ms)	2	30±10	9±8	21±4	14±2	21±6	28±5	30±4
$\%T_{lengthen}$ (% of cycle)	4	41±4	45±4	52±3	55±2	50±2	55±3	67±3
$\%T_{shorten}$ (% of cycle)	4	44±4	39±4	34±3	31±3	37±3	35±3	32±3
ΔL_{max} ($\%L_0$)	4	9±1	15±1	19±1	21±1	20±2	21±2	17±3
ΔL_{min} ($\%L_0$)	4	−7±1	0±2	6±2	4±2	5±2	5±2	5±2

Values are means ± S.E.M.

N_i, number of individuals. For N_i=2, 3 or 4, the number of strides used to calculate means for each speed for each variable ranged from 4 to 8, from 7 to 12 and from 7 to 16, respectively.

$Lag_{Lmax–on}$ is the lag time between EMG onset and maximal muscle length, $\%T_{lengthen}$ and $\%T_{shorten}$ are the percentages of the cycle that the muscle lengthened or shortened, respectively, and ΔL_{max} and ΔL_{min} are maximum and minimum muscle strains, respectively.

See Table 2 and Table 3 for tests of significant variation among locomotor speeds.

Table 2. *Summary of* F*-tests for two-way ANOVAs performed separately for each variable*

Dependent variable	Speed	Individual × speed
Cycle duration	37.2** (5,10)	2.7* (10,38)
EMG duration	11.7** (5,10)	0.8 (10,38)
EMG duty factor	1.9 (5,10)	1.0 (10,38)
EMG relative intensity	6.0* (5,10)	1.3 (10,38)
$Lag_{Lmax–on}$	0.9 (5,5)	5.9** (5,24)
$Lag_{Lmin–off}$	0.6 (5,5)	8.3** (5,24)

*P<0.05; **P<0.001.

Degrees of freedom are indicated in parentheses.

$Lag_{Lmax–on}$ and $Lag_{Lmin–off}$ are the lag times between EMG onset and maximum muscle length and EMG offset and minimum muscle length, respectively.

Table 3. *Summary of* F*-tests for significance of effects in two-way ANOVAs performed separately for each muscle variable*

Dependent variable	Speed d.f.=5,15	Individual × speed d.f.=15,58
ΔL_{max}	5.8*	4.4**
ΔL_{min}	5.0*	6.4**
ΔL_{net}	1.0	5.9**
V	12.9**	1.1
Cycle frequency	75.9**	1.1
$\%T_{shorten}$	2.3	0.6
$\%T_{lengthen}$	2.0	4.0**

*P<0.05; **P<0.001.

ΔL_{max}, ΔL_{min} and ΔL_{net} are the maximum, minimum and net strain, respectively.

V, average shortening velocity of the muscle.

$\%T_{lengthen}$ and $\%T_{shorten}$ are the percentages of the cycle that the muscle lengthened or shortened, respectively.

the muscle strains of the other three individuals changed as negative quadratic functions of locomotor speed.

In contrast to ΔL_{max} and ΔL_{min}, the net muscle strain (ΔL_{net}) showed no regular (Fig. 4C) or significant (Table 3) change with increasing locomotor speed. The estimates of the average relative speed of muscle shortening (V), which were based on values of ΔL_{net}, showed highly significant changes with increasing locomotor speed (Table 3), primarily as a result of the decreased times over which shortening occurred. From 50 to 200 cm s^{-1}, V increased nearly threefold from 1.5 to 4.0 L s^{-1} (Fig. 4D), where L is the resting length of the CF, but little change in V occurred with increased locomotor speeds greater than 200 cm s^{-1}. As was the case with muscle strains, the changes in V could be either a linear or negative quadratic response with increasing locomotor speed, depending on the individual.

The main effect of locomotor speed on the percentages of the cycle spent shortening ($\%T_{shorten}$) and lengthening ($\%T_{lengthen}$) was not significant (Table 3). However, $\%T_{lengthen}$ did have a highly significant speed by individual interaction term (Table 3) partly as a result of both linear and quadratic changes with speed occurring in different individuals. The mean values of $\%T_{shorten}$ and $\%T_{lengthen}$ showed a quite regular pattern of variation with increasing speed (Table 1), such that these two quantities were nearly equal at 50 cm s^{-1} and $\%T_{lengthen}$ tended to be greater than $\%T_{shorten}$ at higher locomotor speeds.

The entire duration of shortening of the CF was generally confined to the stance phase of each stride (Fig. 5). The beginning of muscle shortening relative to the beginning of stance (footfall) did not have any significant (Table 4, $Lag_{Lmax–down}$) or consistent pattern of variation (Fig. 5) with increasing locomotor speed, and the overall (N_s=82) mean value (±S.E.M.) of $Lag_{Lmax–down}$ for the six speeds was 4±1 ms after the beginning of stance. The end of muscle shortening

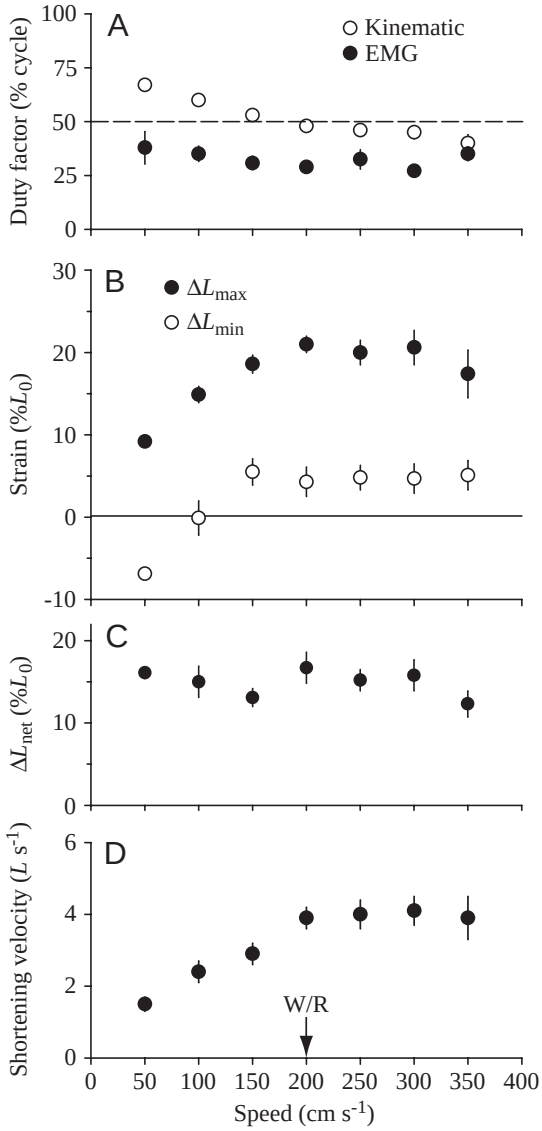

Fig. 4. Mean values (± S.E.M.) of kinematic and electromyographic (EMG) duty factors (A), maximum (ΔL_{max}) and (ΔL_{min}) minimum muscle strain (B), net muscle strain (ΔL_{net}) (C) and average muscle shortening velocity (D) *versus* speed. All values of strain are given as a percentage of resting muscle length (L_0). Mean values were calculated for the total number of strides pooled across three (A) or four (B–D) individuals. W/R, walk–run transition; *L*, resting length of the caudofemoralis muscle.

occurred almost simultaneously with the end of stance at the fastest speed, but the magnitude of $Lag_{Lmin–up}$ increased significantly with decreasing locomotor speeds up to a maximum mean value of −51 ms for the slowest speed (Table 4; Fig. 5). The timing of electrical muscle activity relative to muscle length did not change significantly with speed (Table 2, $Lag_{Lmax–on}$ and $Lag_{Lmin–off}$). The average times ± S.E.M. for which the CF was electrically active began 21±2 ms (N_s=40) prior to maximum length and ended 27±4 ms (N_s=40) before reaching minimum muscle length.

Table 4 includes variables that describe the timing

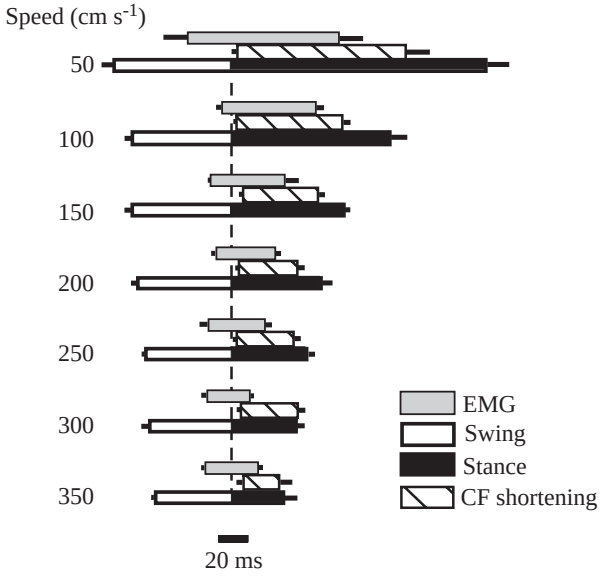

Fig. 5. The mean (± S.E.M.) times of electromyographic (EMG) activity, the beginning of swing, the end of stance and shortening of the caudofemoralis muscle (CF) relative to footfall (dashed vertical line) for each of the speeds of locomotion. For each speed, the top and middle rectangles represent the times of electrical activity of the muscle and muscle shortening, respectively. The bottom rectangle represents the stride cycle, for which the swing and stance phases are indicated by white and black, respectively. Mean values of EMG onset and offset were calculated for the total number of strides pooled across three individuals, and all other variables were calculated for all the strides from four individuals.

relationships between the extreme values of muscle length relative to the extremes of femur rotation, femur retraction and knee extension, none of which changed significantly with increasing speed. Furthermore, the mean values of these lag times were often only a few milliseconds and not significantly different from zero (Table 4). Consequently, the time of L_{max} was nearly synchronous with that of maximal femur protraction, anterior femur rotation and knee extension, and the time of L_{min} was nearly synchronous with that of maximal femur retraction and posterior rotation (Fig. 3).

The tail dorsal angle was effectively constant within a stride cycle (Fig. 3) and, hence, the significant increases in this variable with increasing speed were similar at both the times of L_{max} and L_{min} (Table 5; Fig. 6). Within a stride cycle, the tail lateral angle showed clear periodic change at high speeds but not at low speeds (Fig. 3), and this angle increased significantly with increasing speed at L_{max} but not at L_{min} (Table 5). Tail lateral flexion did not change significantly with speed at either the time of L_{max} (F=0.9, d.f=5,15) or the time of L_{min} (F=0.9, d.f=5,15), and the grand means (± S.E.M., N_s=82) of lateral tail flexion at these times were −4.4±0.6 and 0.8±0.6 °, respectively. The angles of knee and femur depression increased significantly with increasing speed at the time of L_{max} but not at the time of L_{min} (Table 5; Fig. 6). The angle of dorsal tail flexion increased quite steadily over the entire range of seven speeds, whereas the angles of knee and

Table 4. *Summary of* F*-tests and select mean values of lag times (ms) between the extremes of kinematics and muscle length from two-way ANOVAs performed separately for each variable using data from six standardized speeds (50–300 cm s^{-1})*

	ANOVA *F*-values		Mean values ± S.E.M.		
Variable	Speed d.f.=5,15	Individual × speed d.f.=15,58	50 cm s^{-1} (N_s=12)	200 cm s^{-1} (N_s=14)	300 cm s^{-1} (N_s=11)
$Lag_{Lmax–down}$	1.3	1.7	4±2	4±2	7±2
$Lag_{Lmax–antrot}$	2.8	1.1	0±2	0±2	5±2
$Lag_{Lmax–fempro}$	1.1	1.1	10±2	5±2	5±2
$Lag_{Lmax–kext}$	2.3	1.4	1±4	8±3	8±3
$Lag_{Lmin–up}$	7.6**	0.9	–51±11	–20±5	–2±4
$Lag_{Lmin–pstrot}$	1.8	0.5	3±11	–3±4	11±4
$Lag_{Lmin–femret}$	1.6	1.2	–5±10	–7±4	7±4

**P<0.001.

Subscripts of Lmax and down, antrot, fempro, kext indicate lag times between maximum muscle length and the times of footfall, maximum anterior rotation of the femur, maximum femur protraction and maximum knee extension near the time of footfall, respectively.

Subscripts of Lmin and up, pstrot and femret indicate lag times between minimum muscle length and the times of foot-up, maximum posterior rotation of the femur and maximum femur retraction, respectively.

N_s, number of strides.

Table 5. *Summary of* F*-tests and select mean values of kinematic angles (degrees) at the times of maximum and minimum muscle length from two-way ANOVAs performed separately for each variable using data from six standardized speeds (50–300 cm s^{-1})*

	ANOVA *F*-values		Mean values ± S.E.M.		
Variable	Speed d.f.=5,15	Individual × speed d.f.=15,58	50 cm s^{-1} (N_s=12)	200 cm s^{-1} (N_s=14)	300 cm s^{-1} (N_s=11)
TL_{max}					
Femur retraction	0.6	2.8*	–42±2	–46±3	–39±6
Femur rotation	1.3	2.1*	–31±3	–22±2	–32±6
Knee	6.1*	2.9*	61±2	101±4	102±8
Femur depression	6.9*	1.4	–3±2	12±3	17±2
Tail dorsal angle	5.5*	2.5*	–5±1	4±3	7±3
Tail lateral angle	6.1*	1.7	–1±2	9±1	7±2
TL_{min}					
Femur retraction	1.0	1.9*	39±2	31±3	35±4
Femur rotation	0.7	2.5*	–91±3	–97±2	–99±3
Knee	0.2	2.6*	119±3	117±5	119±5
Femur depression	1.2	3.0*	12±2	22±2	16±2
Tail dorsal angle	5.5*	2.2*	–2±1	6±3	11±3
Tail lateral angle	0.5	0.9	2±2	4±2	1±2

*P<0.05.

TL_{max} and TL_{min} indicate the time of maximum and minimum length of the muscle.

N_s, number of strides.

femur depression had the most conspicuous increase from 50 to 200 cm s^{-1} and little regular change with further increases in speed. Femur retraction and femur rotation did not change significantly with increasing speed at either the time of L_{max} or the time of L_{min} (Table 5; Fig. 6).

We used both multiple regressions and supplemental observations to gain further insights in the relationships between individual kinematic variables and muscle strain because isolating the effects of a particular movement on muscle strain was complicated by two sources of intercorrelations among kinematic variables. Joint angles can covary both within a single stride cycle (Fig. 3, femur retraction and rotation) and among different strides as speed increases (Fig. 6). For example, for data pooled from all strides at L_{max} and L_{min} from 50 to 350 cm s^{-1} (N_s=178), all the pairwise combinations of the kinematic variables describing limb position in Table 5 had significant simple Pearson correlation coefficients with P<0.01. Of these kinematic variables, only femur retraction, femur rotation and knee angle had significant simple correlations with muscle strain (r=–0.75, r=–0.69, r=–0.43, respectively, N_s=178, P<0.001). Our final choice of a model predicting muscle strain

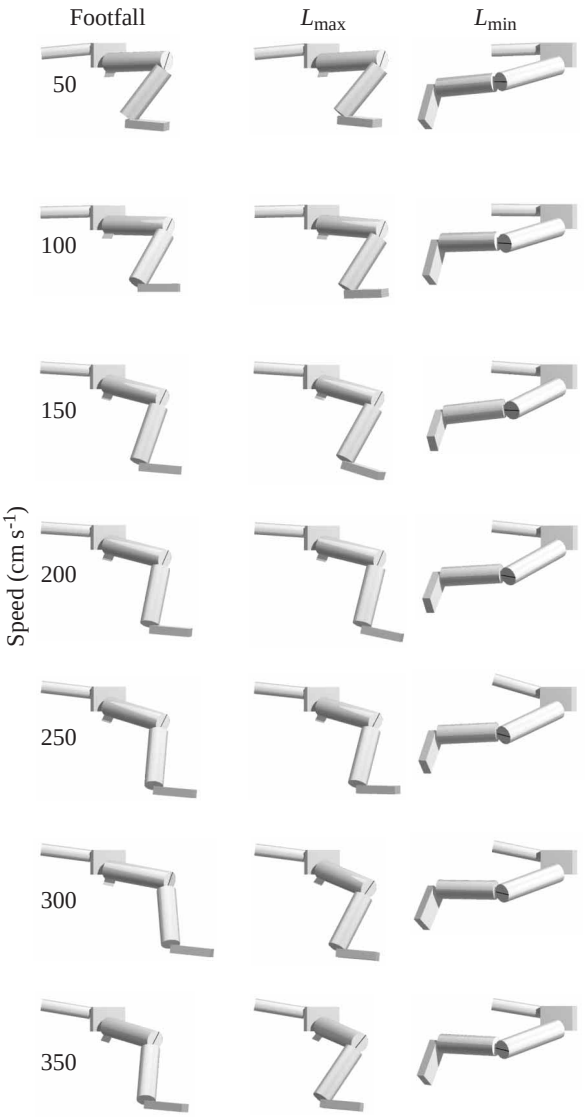

Fig. 6. Schematic right lateral views showing the effects of speed on the kinematics of the hindlimb. The uppermost cylinder in each figure represents the proximal portion of the tail, and the remaining objects are as in Fig. 2, and from proximal to distal represent the pelvis, the femur, the lower leg and the tarsals and metatarsals, respectively. To facilitate comparison of limb positions, the pelvis is shown at the same height within each row of figures, but in the real lizards the height of the pelvis relative to the tread surface did vary significantly within the stance phase. From left to right within each row that represents a different speed of locomotion, the average limb positions are shown at the beginning of stance and at the times of maximal (L_{max}) and minimal (L_{min}) length of the caudofemoralis muscle. Each figure illustrates the mean values (using all strides pooled across four individuals) of the dorsal and lateral angles of the proximal tail and the angles of pelvic rotation, femur retraction, femur rotation, femur depression, knee flexion and ankle flexion. The average times of maximum and minimum muscle length occurred within the stance phase when the foot touches the ground; however, this is not apparent in some figures because the height of the pelvis has been standardized and the toes are not shown.

from kinematics was for the forced-fit multiple regression that simultaneously met the following three criteria: (i) the highest value of r^2, (ii) that each of the partial regression coefficients was significant and (iii) that the sign of each coefficient was consistent with the effects of movement on muscle strain observed from manipulating the anesthetized specimens. Femur retraction and dorsal tail angle both had highly significant (P<0.001) partial regression coefficients in the following model: strain=–0.20(femur retraction)+0.23(dorsal tail angle)+8.02 (r^2=0.60, N_s=178, P≪0.001). Femur retraction had greater importance than dorsal tail angle for predicting muscle strain, as implied by the greater magnitude of its standardized partial regression coefficient (–0.79 *versus* 0.21).

Isolating joint movements by manipulating the limbs of three anesthetized specimens (Fig. 7) consistently showed that the effects of knee extension and femur rotation on muscle strain were strongly dependent on the extent of femur protraction. For example, large cyclic flexions of the knee and moderate rotation of the femur did not affect muscle length when the femur remained markedly retracted (Fig. 7, 0–10 s). The strain of the muscle exceeded resting length only when the knee was anterior to the hip (Fig. 7, 40–80 s, 100–140 s, femur retraction <0 °). When the knee was anterior to the hip and the amounts of femur rotation and knee movement were minimal, protracting and retracting the femur were sufficient to produce large amounts of muscle lengthening and shortening, respectively (Fig. 7, 40–80 s). Large amounts of knee extension produced peak strains of less than 3 % (Fig. 7, 90–100 s) when the femur was only slightly protracted (<5 °) and produced peak strains exceeding 20 % (Fig. 7, 110–130 s) while the femur remained maximally protracted (45 °). Pronounced knee flexion while the femur remained maximally protracted (Fig. 7, 110–130 s) only decreased muscle strain to those values observed for isolated femur protraction (Fig. 7, 40–80 s) rather than allowing the muscle to return to its resting length.

Discussion

Speed had pervasive effects on the time course and intensity of muscle activity, the kinematics of the hind limb and the maximum and minimum length of the CF muscle. Rather than a simple linear increase with increasing speed, several variables measured in this study increased from the slowest speed up to the walk–run transition (duty factor 50 %) but changed little with further increases in speed. The maximal sprinting speeds of adult *Dipsosaurus dorsalis* tested (Marsh, 1988) in the laboratory at 40 °C range from approximately 3 to 5 m s^{-1}, and scaling equations (Marsh, 1988) predict an average maximal sprinting speed of 3.6 m s^{-1} for the animals used in our study. The maximum aerobically sustainable speed of *D. dorsalis* is approximately 30 cm s^{-1} (John-Alder and Bennett, 1981). Consequently, we used a range of speeds that nearly spans the range that is physiologically possible for this species, but none of the standardized speeds that we used appears to be aerobically sustainable.

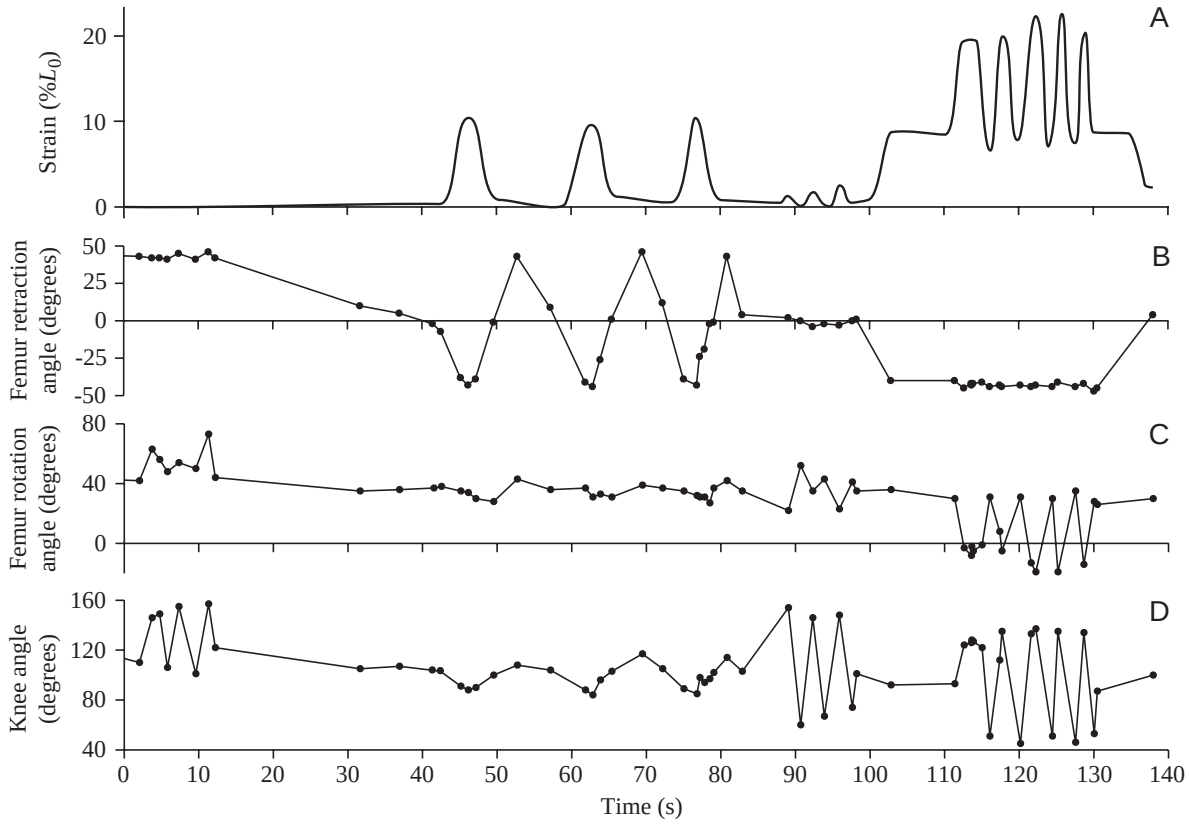

Fig. 7. Effects of femur retraction (B), femur rotation (C) and knee angle (D) on the length (A) of the caudofemoralis muscle of a *Dipsosaurus dorsalis*. The data shown are from one of the three individuals for which the hindlimb was manipulated while the lizard was anesthetized. The strain of the caudofemoralis muscle is expressed as a percentage change from its resting length (L_0).

Muscle fiber type

The caudofemoralis muscle (CF) of *Dipsosaurus dorsalis* has three major fiber types: fast glycolytic, fast oxidative glycolytic and slow twitch, which comprise 72 %, 24 % and 4 % of the cross-sectional area, respectively (Putnam et al., 1980). Red regions in the skeletal muscles of lizards commonly include substantial portions of both fast oxidative glycolytic and slow-twitch fibers, whereas white regions have almost exclusively fast glycolytic fibers (Gleeson et al., 1980).

Differences in muscle fiber type are correlated with differences in (i) the speed at which muscle fibers are recruited, (ii) how EMG amplitude changes with increasing speed and (iii) the timing of EMGs. For example, aerobically sustainable locomotion of lizards probably involves activity of only the red region fibers (Jayne et al., 1990a), as is the case for the swimming of many species of fishes (for reviews, see Bone et al., 1978; Rome et al., 1984). The EMG electrodes in some but not all of the individuals of *D. dorsalis* detected CF activity during irregular bouts of locomotion (not analyzed quantitatively) that were slow enough to be sustainable. During the terrestrial locomotion of monitor lizards, EMGs from a red region of a limb muscle increase in intensity up to an intermediate speed, after which little change is apparent with further increases in speed (Jayne et al., 1990a). For some individuals of *D. dorsalis*, we found a similar pattern for the EMGs from the electrodes that detected activity at the slowest speeds, but the EMG intensities increased over the entire range of increased speed in other individuals. At certain speeds, the onset of EMG activity in the red fibers precedes that in the faster white fibers in some species of teleost fishes (Coughlin and Rome, 1996; Gillis, 1998; Jayne and Lauder, 1994), and this is similar to the timing differences between the electrode in each *D. dorsalis* that was operationally defined as being in the slowest fiber type and the other electrodes in the same caudofemoralis muscle. Therefore, the EMGs that we analyzed quantitatively were from electrodes that appeared to detect activity from slow twitch or fast oxidative glycolytic fibers, but some electrodes also appeared to be detecting activity from additional faster fiber types.

The contractile properties determined from *in vitro* studies allow one to predict when the CF developed force during our *in vivo* experiments which were performed near a temperature of 40 °C. For isometric twitches of the iliofibularis muscle of *D. dorsalis* at 40 °C, the time from the onset of force development to peak tension for the red region is only slightly longer than that for the white region (25 *versus* 21 ms), whereas the time from peak tension to half-relaxation of the red region is considerably longer than that of the white region (28 *versus* 18 ms) (Gleeson et al., 1980). The graphical data of Johnson et al. (Johnson et al., 1993) for *D. dorsalis* suggest that the time

from half-relaxation to complete relaxation generally exceeds the time from peak tension to half-relaxation time. Thus, conservative estimates of the minimal times to complete relaxation of red and white muscle of *D. dorsalis* at 40 °C are approximately 56 and 36 ms, respectively.

Comparisons with previous EMG and kinematic studies of tetrapods

As a result of sharing a fundamentally sprawling limb posture, many similarities in limb function are likely for salamanders, alligators and lizards (Ashley-Ross, 1994a; Barclay, 1946; Gatesy, 1991; Reilly and Delancey, 1997; Rewcastle, 1981), but these groups have some important differences in morphology. For example, the auxiliary tendon of the CF that extends to the knee of alligators and lizards (Fig. 1) is absent from salamanders and birds. Consequently, although many insights into limb function can be gained by comparing vertebrate taxa with sprawling limbs, the additional joint spanned by the CF in alligators and lizards could result in the functions of this muscle in salamanders being only a subset of the functions that are possible in alligators and lizards.

The CF of *Dipsosaurus dorsalis* was active during late swing and early stance (Fig. 5), which is grossly similar to the findings of previous studies of alligators and lizards (Gatesy, 1997; Reilly, 1995). In contrast to these reptiles, the onset of CF activity occurs after the beginning of stance by approximately 50 % of the duration of stance in birds (Gatesy, 1999) and by approximately 20 % of the duration of stance in salamanders (Ashley-Ross, 1995; Peters and Goslow, 1983). The offset of CF activity for *D. dorsalis* occurs slightly before mid-stance (38 % of stance duration), whereas the offset of activity is after mid-stance for salamanders (64–70 %), fence lizards (59 %), alligators (76 %) and birds (70–75 %) (Ashley-Ross, 1995; Gatesy, 1997; Gatesy, 1999; Peters and Goslow, 1983; Reilly, 1995).

In *D. dorsalis*, the onset of CF activity averaged 21 ms before the time of L_{max}, which occurred an average of 4 ms after footfall. At all speeds for *D. dorsalis*, the average times of maximal knee extension, maximal femur protraction and maximal anterior femur rotation were nearly synchronous (often within 4 ms) with L_{max}. The short times for developing force in the skeletal muscle of *D. dorsalis* (21–25 ms) (Gleeson et al., 1980) and the potential of stretch activation to decrease these times suggest that the CF of *D. dorsalis* could contribute to retarding femur protraction, anterior femur rotation and knee extension near the end of the swing phase.

The CF activity in the alligator prior to footfall (Gatesy, 1990; Gatesy, 1997) may facilitate retardation of knee extension in a fashion similar to that in lizards, but the absence of a CF insertion on the crus in salamanders and birds precludes a similar function. In contrast to lizards and alligators, the onset of CF activity in salamanders and birds occurs too late to facilitate this reversal of femur protraction during late swing.

The average time between L_{min} and the offset of CF activity ($Lag_{Lmin–off}$) was 27 ms, and the lag times between CF offset and maximum femur retraction and posterior rotation were similar to $Lag_{Lmin–off}$. Thus, the offset of CF activity corresponds closely to the cessation of femur retraction and posterior rotation after correcting for the likely relaxation time (Gleeson et al., 1980; Johnson et al., 1993).

The flexion of the knee during early to mid-swing in *D. dorsalis* is not caused by the CF because it lengthens during this time. This emphasizes how, when the knee is posterior to the hip, the angle of the knee is irrelevant to strain of the CF.

While the foot contacts the ground, the forward momentum of a lizard moving steadily could move the limb posteriorly (Snyder, 1954). Similarly, the impact of landing tends to flex the knee during early stance when the ground reaction force is oriented such that it exerts a braking effect (Farley and Ko, 1997). Consequently, one cannot rule out the possibility that these passive mechanisms contribute to the limb movements of *D. dorsalis*. However, during stance of *D. dorsalis*, the timing of CF activity and shortening are consistent with the muscle actively causing femur retraction and posterior femoral rotation nearly throughout stance and causing knee flexion during early stance. The gross pattern of CF activity in salamanders, fence lizards, alligators and birds is also consistent with actively retracting the femur (Ashley-Ross, 1995; Gatesy, 1997; Gatesy, 1999; Peters and Goslow, 1983; Reilly, 1995).

Besides the functions of the caudofemoralis for limb movement, both Peters and Goslow (Peters and Goslow, 1983) and Gatesy (Gatesy, 1990) suggested that the CF of ectothermic tetrapods moves the tail laterally towards the side of the active muscle. Gatesy (Gatesy, 1990) also suggested that the CF contributes to undulating the tail laterally. Lateral undulations are generally regarded as a combination of lateral displacement of axial structures and lateral flexion. In this study of *D. dorsalis*, the lateral tail angle best indicates lateral movement, whereas the angle of lateral flexion indicates localized lateral bending.

Contrary to one hypothesized function of the CF (Gatesy, 1990; Peters and Goslow, 1983), when the tail of *D. dorsalis* had detectable lateral movement, it was away from the side of CF activity (Fig. 3, Fig. 8). When lateral flexion of the tail was detectable, the tail changed from being convex to concave towards the side of CF activity (Fig. 8) in a manner consistent with active bending caused by the CF. However, the activity of the CF and nearby axial muscles in the base of the tail are out of phase (Jayne and Daggy, 2000; Reilly, 1995; and preliminary results from this study). Similar to our findings for *D. dorsalis*, midline diagrams of a fence lizard at the onset of CF activity indicate that the tail is convex and pointed towards the side of activity (Reilly, 1995), but similar data are lacking for alligators and salamanders (Ashley-Ross, 1995; Gatesy, 1997; Gatesy, 1999; Peters and Goslow, 1983).

Integrating in vivo *muscle activity with* in vitro *muscle physiology*

Several factors that are intrinsic and extrinsic to the muscle

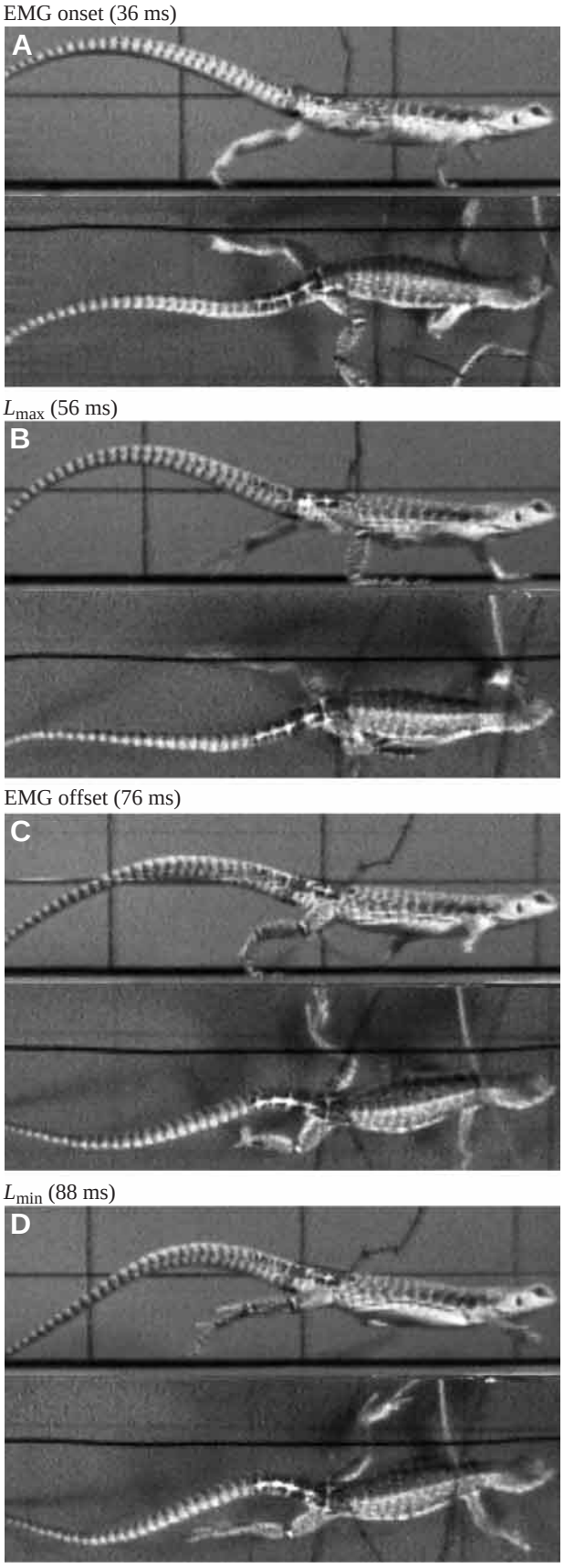

Fig. 8. Simultaneous lateral and dorsal views of a *Dipsosaurus dorsalis* running at 350 cm s^{-1} at the beginning (A) and end (C) of electrical activity and at the maximum (L_{max}; B) and minimum (L_{min}; D) length of the right caudofemoralis muscle. The images are from the same sequence as shown in Fig. 3C, and the time elapsed since the beginning of the swing phase (foot-up) of the right hind limb is given above each panel. The base of the tail moves away from the side of caudofemoralis activity.

affect its force production and power output during cyclical loading. For example, differences in contractile kinetics are associated with different fiber types. Furthermore, the mechanical output of muscle may change with cycle frequency, muscle length, shortening velocity, the timing of muscle activation relative to strain and the proportions of the cycle spent lengthening and shortening.

In our study of *D. dorsalis*, the mean durations of the limb cycles (253–96 ms) and their corresponding frequencies showed nearly threefold variation (3.9–10.4 Hz). Such large variation in the time course of events can affect the power produced by muscle and whether or not the muscle is able to relax completely between successive cycles. The power output during *in vitro* work loops of fast glycolytic fibers from the iliofibularis muscle of large *D. dorsalis* is maximized at a frequency of approximately 10 Hz and declines at higher frequencies partly because the muscle does not relax completely (Johnson et al., 1993; Swoap et al., 1993). In our experiments, the mean EMG duration at 350 cm s^{-1} was 33 ms and, when added to the times to complete relaxation for red (56 ms) and white (36 ms) muscle from *D. dorsalis* (Gleeson et al., 1980; Johnson et al., 1993), the resulting times (89 and 69 ms) are less than the cycle duration of the fastest speed. Consequently, at the fastest running speed of *D. dorsalis*, complete relaxation of both slow and fast fibers seems likely.

The CF of *D. dorsalis* is unlikely to be functioning only on the plateau of the sarcomere length/tension curve where isometric force is maximized (Gordon et al., 1966) because of the significant changes in ΔL_{max} and ΔL_{min} with increasing locomotor speed. The plateau of the sarcomere length/tension curve extends over a range of strain of less than 10 % of the resting sarcomere length (Gordon et al., 1966). Consequently, if the CF strains of *D. dorsalis* at low speeds encompass the plateau of the sarcomere length/tension curve, the greater values of ΔL_{min} at speeds of 150 cm s^{-1} and above could be sufficiently large to shift the strain cycle and eliminate any overlap with the region of the sarcomere length/tension curve where force is maximized. In contrast to the CF of *D. dorsalis*, the amplitudes of ΔL_{max} and ΔL_{min} of the axial muscles of steadily swimming fishes have equal and opposite amplitudes that increase with increasing speed and, hence, always overlap the plateau of the sarcomere length/tension curve (Coughlin, 2000; Rome, 1994).

With increasing speed of locomotion for *Dipsosaurus dorsalis*, increased elevation of the tail is probably a major factor contributing to the increases in both ΔL_{max} and ΔL_{min} of the CF. Although the joint angles within the limb change periodically

during steady locomotion, the dorsal tail angle can remain effectively constant within a stride cycle. Thus, postural changes in the tail may be an important mechanism for modulating muscle strain that is largely independent of limb movements.

The average shortening velocity of the CF increased with locomotor speed in *Dipsosaurus dorsalis* as a result of the decreased duration of shortening rather than changes in net strain. Hill (Hill, 1938) suggested that muscle produces maximal power by shortening over a small range (0.2–0.4) of V/V_{max}. The maximum shortening velocities (V_{max}) of *D. dorsalis* fast-twitch glycolytic, fast-twitch oxidative glycolytic and slow-twitch oxidative fibers are 18.7, 7.1 and $2.8\,L\,s^{-1}$, respectively (Gleeson and Johnston, 1987; Marsh and Bennett, 1985). For locomotor speeds from 50 to $200\,cm\,s^{-1}$, average shortening velocity increased from 1.5 to $3.9\,L\,s^{-1}$; hence, from the fastest to the slowest fiber type, this represents 0.08–0.21, 0.21–0.56 and 0.54–1.4V/V_{max}, respectively. The slowest CF fibers in *D. dorsalis* cannot contribute to force production during shortening at locomotor speeds above $150\,cm\,s^{-1}$ because V/V_{max} exceeds 1, and several additional values of V/V_{max} were outside the expected optimal range. Electrical activity of the fastest muscle fiber type in the CF was generally confined to locomotor speeds that exceeded $200\,cm\,s^{-1}$, at which the values of V/V_{max} (0.21) were similar to the optimal range predicted by Hill (Hill, 1938).

The work-loop method provides an alternative for determining the shortening velocity of muscle that maximizes power by loading muscle cyclically and varying the strain and pattern of stimulation until power output is maximized. Contrary to the narrow optimal range of V/V_{max} predicted by Hill (Hill, 1938), Askew and Marsh (Askew and Marsh, 1998) found that a large range (0.075–0.30) of V/V_{max} can optimize power depending on the frequency of cyclical loading and the amount of time spent shortening. However, many values of V/V_{max} observed for the slower fibers in the CF of *D. dorsalis* are also outside the large range of values found by Askew and Marsh (Askew and Marsh, 1998).

Work-loop experiments have also demonstrated that the power output of a muscle is affected by changes in the phase of muscle stimulation relative to the strain cycle (Josephson, 1999). Rather than having a constant phase relationship between EMG onset and the strain cycle, the lag time between onset of CF activity and the initiation of muscle shortening was constant (grand mean $Lag_{Lmax-on}$=21 ms) and nearly coincident with the time to peak twitch tension (21–25 ms, Gleeson et al., 1980). As a result of the decreased cycle duration, the corresponding phase lags (lag time divided by cycle duration) more than doubled (8–21 % of a cycle) as speed increased from 50 to $350\,cm\,s^{-1}$. Similar speed-induced phase shifts between EMG activity and muscle strain also occur in other rhythmic locomotor behaviors as speed increases (Coughlin et al., 1996; Jayne and Lauder, 1995). Work-loop experiments with the caudofemoralis would be useful for determining how much negative work might be performed by the CF in the 20 ms preceding L_{max}.

Most previous work-loop experiments have used simple sinusoidal or saw-toothed patterns of strain for which the times of lengthening and shortening are equal (for a review, see Marsh, 1999). For the undulatory swimming of fishes, such symmetrical changes in strain closely approximate *in vivo* conditions over a wide range of steady speeds (Coughlin et al., 1996). However, a striking difference between limbed and axial locomotor movements is that, as the speed of limbed locomotion increases, the propulsive (stance) proportion of the cycle decreases significantly. Thus, for limbed locomotion, even if the speed of muscle shortening were constant over the entire propulsive phase, the change in duty factor that occurs with changing speed is likely to cause a temporal asymmetry in the strain cycle experienced by a muscle.

In the light of the naturally asymmetric strain regimes of muscle, Askew and Marsh (Askew and Marsh, 1998) performed work-loop experiments in which manipulating the symmetry of the strain cycle revealed that increasing the shortening portion of the cycle generally increases power output when other factors are held constant. Furthermore, previous *in vivo* studies of scallop swimming (Marsh et al., 1992), bird flight (Biewener et al., 1998a) and frog calling (Girgenrath and Marsh, 1997) have found muscle strain cycles with longer periods of shortening rather than lengthening. In contrast, the *in vivo* strain cycle of the CF muscle of *D. dorsalis* often had greater periods of lengthening rather than shortening. Additional muscles that actively cause limb movement during stance are likely to spend more time lengthening than shortening because the duration of stance is less than that of swing during running. These combined observations of *in vivo* muscle strain demonstrate an impressive diversity of muscle function that would be difficult to predict from a few relatively simple optimizing criteria. Consequently, as emphasized by Askew and Marsh (Askew and Marsh, 1998), future *in vitro* studies of muscle physiology that integrate *in vivo* data are particularly promising for gaining a comprehensive understanding of muscle function.

This research was supported by NSF grants IBN 9514585 to B.C.J. and IBN-9983003 to B.C.J. and D.I. The acquisition of a high-speed video system and a sonomicrometry system was supported by NSF grant BIR 9217409 and a University of Cincinnati University Research Council Grant for Faculty Development, respectively, to B.C.J. We thank Richard Marsh for his assistance in teaching us how to implant sonomicrometry crystals and use the sonomicrometry system. We also thank R. German and D. Gist and T. Roberts for their suggestions on the manuscript. J. Rodenburg helped to collect the lizards used for the research. D. Scovill of the Mojave National Preserve and J. Brode of California Fish and Game provided timely processing of our permit applications. The facilities of the Sweeney Granite Mountains Desert Research Center facilitated the collection of animals.

References

Abraham, L. D. and Loeb, G. E. (1985). The distal hindlimb musculature of the cat. *Exp. Brain Res.* **58**, 580–593.

Altringham, J. D., Wardle, C. S. and Smith, C. I. (1993). Myotomal muscle function at different locations in the body of a swimming fish. *J. Exp. Biol.* **182**, 191–206.

Ashley-Ross, M. A. (1994a). Hind limb kinematics during terrestrial locomotion in a salamander (*Dicamptodon tenebrosus*). *J. Exp. Biol.* **193**, 255–283.

Ashley-Ross, M. A. (1994b). Metamorphic and speed effects on hind limb kinematics during terrestrial locomotion in the salamander *Dicamptodon tenebrosus*. *J. Exp. Biol.* **193**, 285–305.

Ashley-Ross, M. A. (1995). Patterns of hind limb motor output during walking in the salamander *Dicamptodon tenebrosus*, with comparisons to other tetrapods. *J. Comp. Physiol. A* **177**, 273–285.

Askew, G. N. and Marsh, R. L. (1998). Optimal shortening velocity (V/V_{max}) of skeletal muscle during cyclical contractions: length–force effects and velocity-dependent activation and deactivation. *J. Exp. Biol.* **201**, 1527–1540.

Barclay, O. R. (1946). The mechanics of amphibian locomotion. *J. Exp. Biol.* **23**, 177–203.

Biewener, A. (1990). Biomechanics of mammalian terrestrial locomotion. *Science* **250**, 1097–1103.

Biewener, A. A., Corning, W. R. and Toblaske, B. W. (1998a). *In vivo* pectoralis muscle force–length behavior during level flight in pigeon (*Columba livia*). *J. Exp. Biol.* **201**, 3293–3307.

Biewener, A. A., Konieczynski, D. D. and Baudinette, R. V. (1998b). *In vivo* muscle force–length behavior during steady-speed hopping in Tammar wallabies. *J. Exp. Biol.* **201**, 1681–1694.

Bone, Q., Kiceniuk, J. and Jones, D. R. (1978). On the role of the different fibre types in fish myotomes at intermediate swimming speeds. *Fish. Bull.* **76**, 691–699.

Brinkman, D. (1981). The hind limb step cycle of *Iguana* and primitive reptiles. *J. Zool., Lond.* **181**, 91–103.

Carrier, D. R., Gregersen, C. S. and Silverton, N. A. (1998). Dynamic gearing in running dogs. *J. Exp. Biol.* **201**, 3185–3195.

Coughlin, D. J. (2000). Power production during steady swimming in largemouth bass and rainbow trout. *J. Exp. Biol.* **203**, 617–629.

Coughlin, D. J. and Rome, L. C. (1996). The roles of pink and red muscle in powering steady swimming in scup, *Stenotomus chrysops*. *Am. Zool.* **36**, 666–677.

Coughlin, D. J., Valdes, L. and Rome, L. C. (1996). Muscle length changes during swimming in scup: sonomicrometry verifies the anatomical cine technique. *J. Exp. Biol.* **199**, 459–463.

Edwards, J. L. (1977). The evolution of terrestrial locomotion. In *Major Patterns in Vertebrate Evolution* (ed. M. K. Hecht, P. C. Goody and B. M. Hecht), pp. 553–576. New York: Plenum Publishing Corp.

Farley, C. T. and Ko, T. C. (1997). Mechanics of locomotion in lizards. *J. Exp. Biol.* **200**, 2177–2188.

Fieler, C. L. and Jayne, B. C. (1998). Effects of speed on the hindlimb kinematics of the lizard *Dipsosaurus dorsalis*. *J. Exp. Biol.* **201**, 609–622.

Full, R. J., Stokes, D. R., Ahn, A. N. and Josephson, R. K. (1998). Energy absorption during running by leg muscles in a cockroach. *J. Exp. Biol.* **201**, 997–1012.

Gatesy, S. M. (1990). Caudofemoral musculature and the evolution of theropod locomotion. *Paleobiology* **16**, 170–186.

Gatesy, S. M. (1991). Hind limb movements of the American alligator (*Alligator mississippiensis*) and postural grades. *J. Zool., Lond.* **224**, 577–588.

Gatesy, S. M. (1997). An electromyographic analysis of hindlimb function in *Alligator* during terrestrial locomotion. *J. Morph.* **234**, 197–212.

Gatesy, S. M. (1999). Guineafowl hind limb function. II. Electromyographic analysis and motor pattern evolution. *J. Morph.* **240**, 127–142.

Gillis, G. B. (1998). Neuromuscular control of anguilliform locomotion: patterns of red and white muscle activity during swimming in the American eel *Anguilla rostrata*. *J. Exp. Biol.* **201**, 3245–3256.

Girgenrath, M. and Marsh, R. L. (1997). *In vivo* performance of trunk muscles in tree frogs during calling. *J. Exp. Biol.* **200**, 3101–3108.

Gleeson, T. T. (1983). A histochemical and enzymatic study of the muscle fiber types in the water monitor, *Varanus salvator*. *J. Exp. Zool.* **227**, 191–201.

Gleeson, T. T. and Dalessio, P. M. (1990). Lactate: a substrate for reptilian muscle gluconeogenesis following exhaustive exercise. *J. Comp. Physiol. B* **160**, 331–338.

Gleeson, T. T., Dalessio, P. M., Carr, J. A., Wickler, S. J. and Mazzeo, R. S. (1993). Plasma catecholamine and corticosterone concentrations and their *in vitro* effects on lizard skeletal muscle lactate metabolism. *Am. J. Physiol.* **265**, R632–R639.

Gleeson, T. T. and Johnston, I. A. (1987). Reptilian skeletal muscle: contractile properties of identified single fast-twitch and slow fibers from the lizard *Dipsosaurus dorsalis*. *J. Exp. Zool.* **242**, 283–290.

Gleeson, T. T., Putnam, R. W. and Bennett, A. F. (1980). Histochemical, enzymatic and contractile properties of skeletal muscles fibers in the lizard, *Dipsosaurus dorsalis*. *J. Exp. Zool.* **214**, 293–302.

Gordon, A. M., Huxley, A. F. and Julian, F. J. (1966). The variation in isometric tension with sarcomere length in vertebrate muscle fibres. *J. Physiol., Lond.* **184**, 170–192.

Hildebrand, M. (1985). Walking and running. In *Functional Vertebrate Morphology* (ed. M. Hildebrand, D. M. Bramble, K. F. Liem and D. B. Wake), pp. 38–57. Cambridge, MA: Belknap Press of Harvard University Press.

Hill, A. V. (1938). The heat of shortening and the dynamic constants of muscle. *Proc. R. Soc. Lond. B* **126**, 136–195.

Irschick, D. J. and Jayne, B. C. (1999a). Comparative three-dimensional kinematics of the hindlimb for high-speed bipedal and quadrupedal locomotion of lizards. *J. Exp. Biol.* **202**, 1047–1065.

Irschick, D. J. and Jayne, B. C. (1999b). A field study of effects of incline on the escape locomotion of a bipedal lizard, *Callisaurus draconoides*. *Physiol. Biochem. Zool.* **72**, 44–56.

Jayne, B. C. (1988). Muscular mechanisms of snake locomotion: an electromyographic study of the sidewinding and concertina modes of *Crotalus cerastes*, *Nerodia fasciata* and *Elaphe obsoleta*. *J. Exp. Biol.* **140**, 1–33.

Jayne, B. C., Bennett, A. F. and Lauder, G. V. (1990a). Muscle recruitment during terrestrial locomotion: how speed and temperature affect fibre type use in a lizard. *J. Exp. Biol.* **152**, 101–128.

Jayne, B. C. and Daggy, M. W. (2000). The effects of temperature on the burial performance and axial motor pattern of the sand-swimming of the Mojave fringe-toed lizard, *Uma scoparia*. *J. Exp. Biol.* **203**, 1241–1252.

Jayne, B. C. and Ellis, R. V. (1998). How inclines affect the escape behaviour of a dune dwelling lizard, *Uma scoparia*. *Anim. Behav.* **55**, 1115–1130.

Jayne, B. C. and Irschick, D. J. (1999). Effects of incline and speed on the three-dimensional hindlimb kinematics of a generalized iguanian lizard (*Dipsosaurus dorsalis*). *J. Exp. Biol.* **202**, 143–159.

Jayne, B. C. and Lauder, G. V. (1994). How fish use slow and fast muscle fibers: implications for models of vertebrate muscle recruitment. *J. Comp. Physiol. A* **175**, 123–131.

Jayne, B. C. and Lauder, G. V. (1995). Red muscle motor patterns during steady swimming in largemouth bass: effects of speed and correlations with axial kinematics. *J. Exp. Biol.* **198**, 1575–1587.

Jayne, B. C., Lauder, G. V., Reilly, S. M. and Wainwright, P. C. (1990b). The effect of sampling rate on the analysis of digital electromyograms from vertebrate muscle. *J. Exp. Biol.* **154**, 557–565.

John-Alder, H. B. and Bennett, A. F. (1981). Thermal dependence of endurance and locomotory energetics in a lizard. *Am. J. Physiol.* **241**, R342–R349.

Johnson, T. P., Swoap, S. J., Bennett, A. F. and Josephson, R. K. (1993). Body size, muscle power output and limitations on burst locomotor performance in the lizard *Dipsosaurus dorsalis*. *J. Exp. Biol.* **174**, 199–213.

Johnston, I. A. and Gleeson, T. T. (1984). Thermal dependence of contractile properties of red and white fibers isolated from the iliofibularis muscle of the desert iguana (*Dipsosaurus dorsalis*). *J. Exp. Biol.* **113**, 123–132.

Josephson, R. K. (1999). Dissecting muscle power output. *J. Exp. Biol.* **202**, 3369–3375.

Marsh, R. L. (1988). Ontogenesis of contractile properties of skeletal muscle and sprint performance in the lizard *Dipsosaurus dorsalis*. *J. Exp. Biol.* **137**, 119–139.

Marsh, R. L. (1999). How muscles deal with real-world loads: The influence of length trajectory on muscle performance. *J. Exp. Biol.* **202**, 3377–3385.

Marsh, R. L. and Askew, G. N. (1998). The mechanical power output of quail pectoralis muscle. *Am. Zool.* **38**, 151A.

Marsh, R. L. and Bennett, A. F. (1985). Thermal dependence of isotonic contractile properties of skeletal muscle and sprint performance of the lizard *Dipsosaurus dorsalis*. *J. Comp. Physiol. B* **155**, 541–551.

Marsh, R. L. and Bennett, A. F. (1986). Thermal dependence of contractile properties of skeletal muscle from the lizard *Sceloporus occidentalis* with comments on methods for fitting and comparing force–velocity curves. *J. Exp. Biol.* **126**, 63–77.

Marsh, R. L., Olson, J. M. and Guzik, S. K. (1992). Mechanical performance of scallop adductor muscle during swimming. *Nature* **357**, 411–413.

Peters, S. E. and Goslow, G. E. J. (1983). From salamanders to mammals: continuity in musculoskeletal function during locomotion. *Brain Behav. Evol.* **22**, 191–197.

Putnam, R. W., Gleeson, T. T. and Bennett, A. F. (1980). Histochemical determination of the fiber composition of locomotory muscles in a lizard *Dipsosaurus dorsalis*. *J. Exp. Zool.* **214**, 303–309.

Reilly, S. M. (1995). Quantitative electromyography and muscle function of the hind limb during quadrupedal running in the lizard *Sceloporus clarki*. *Zool. Anal. Complex Syst.* **98**, 263–277.

Reilly, S. M. and Delancey, M. J. (1997). Sprawling locomotion in the lizard *Sceloporus clarkii*: quantitative kinematics of a walking trot. *J. Exp. Biol.* **200**, 753–765.

Rewcastle, S. C. (1981). Stance and gait in tetrapods: an evolutionary scenario. In *Vertebrate Locomotion* (ed. M. H. Day), pp. 239–267. London: Academic Press.

Roberts, T. J., Marsh, R. L., Weyland, P. G. and Taylor, C. R. (1997). Muscular force in running turkeys: the economy of minimizing work. *Science* **275**, 1113–1115.

Rome, L. C. (1994). The mechanical design of the muscular system. *Adv. Vet. Comp. Med.* **38A**, 125–179.

Rome, L. C., Loughna, P. T. and Goldspink, G. (1984). Muscle fiber activity in carp as a function of swimming speed and muscle temperature. *Am. J. Physiol.* **16**, R272–R279.

Snyder, R. C. (1954). The anatomy and function of the pelvic girdle and hindlimb in lizard locomotion. *Am. J. Anat.* **95**, 1–46.

Snyder, R. C. (1962). Adaptations for bipedal locomotion of lizards. *Am. Zool.* **2**, 191–203.

Sukhanov, V. B. (1974). General system of symmetrical locomotion of terrestrial vertebrates and some features of movement of lower tetrapods. New Delhi: Amerind Publ. Co. Pvt. Ltd.

Swoap, S. J., Johnson, T. P., Josephson, R. K. and Bennett, A. F. (1993). Temperature, muscle power output and limitations on burst locomotor performance of the lizard *Dipsosaurus dorsalis*. *J. Exp. Biol.* **174**, 185–197.

Wilkinson, L. (1992). *SYSTAT for Windows: Statistics, Version 5 Edition*. Evanston, IL: SYSTAT Inc.

Zar, J. H. (1999). *Biostatistical Analysis*. Upper Saddle River, NJ: Prentice Hall, Inc.